1782 *Chem. Mater.* **2010,** *22,* 1782–1787
DOI:10.1021/cm903287u

CHEMISTRY OF MATERIALS
Article

Patterned Growth of Boron Nitride Nanotubes by Catalytic Chemical Vapor Deposition

Chee Huei Lee, Ming Xie, Vijaya Kayastha, Jiesheng Wang, and Yoke Khin Yap*

Department of Physics, Michigan Technological University 1400 Townsend Drive, Houghton, Michigan 49931, USA

Received October 27, 2009. Revised Manuscript Received December 21, 2009

For the first time, patterned growth of boron nitride nanotubes is achieved by catalytic chemical vapor deposition (CCVD) at 1200 °C using MgO, Ni, or Fe as the catalysts, and an Al_2O_3 diffusion barrier as underlayer. The as-grown BNNTs are clean, vertically aligned, and have high crystallinity. Near band-edge absorption ~6.0 eV is detected, without significant sub-band absorption centers. Electronic transport measurement confirms that these BNNTs are perfect insulators, applicable for future deep-UV photoelectronic devices and high-power electronics.

The unique structural, mechanical, electronic, and optical properties of carbon nanotubes (CNTs) have attracted tremendous research interest.[1,2] CNTs can be semiconducting or semimetallic, depending on their structures. The small band gap of CNTs makes them applicable for optical devices in the long visible wavelengths and near-IR regions.[3] On the other hand, boron nitride nanotubes (BNNTs) exhibit extraordinary mechanical property like CNTs because of their hexagonal boron nitride (h-BN) network, which is similar to the graphene shells on CNTs. BNNTs therefore become attractive as insulating nanocomposites for mechanical and reinforcement applications. In addition, BNNTs are wide band gap materials (theoretically ~5.0 eV), which are insensitive to the number of walls, diameters, and chiralities.[4] This means they are uniform in electronic properties. Theories predict that BNNTs could have tunable band gap by doping[5] or by applying the Stark effect.[6] These unique electronic properties making BNNTs useful in many applications, such as deep-UV photoelectronic devices, high-temperatures, and high-power electronics. However, the synthesis of BNNTs is much more difficult as compared to that of CNTs. For example, the growth of BNNTs requires high temperatures and the growth location and growth orientation of BNNTs are still uncontrollable. These problems have prevented progressive investigation on the properties and applications of BNNTs.

BNNTs have been synthesized by various methods, including arc-discharge,[7] laser vaporization,[8,9] BN substitution method from CNT templates,[10] chemical vapor deposition (CVD) using borazine,[11,12] induction heating boron oxide CVD (BOCVD),[13,14] ball milling,[15] combustion of FeN/B powders,[16] and templating polymer thermolysis.[17] Among these synthesis techniques, a significant progress has been produced by BOCVD for the mass production of multiwall BNNTs and has led to potential applications.[18,19] BOCVD requires an induction furnace with specific design for achieving high growth temperature (usually 1300−1500 °C) and high temperature gradient. Si-based substrates cannot be used for the coating of BNNTs using this BOCVD approach. Recently, we show that BNNTs can be directly grown on substrates by a plasma-enhanced pulsed-laser deposition

*Corresponding author. E-mail: ykyap@mtu.edu Tel: (906) 487-2900. Fax: (906) 487-2933.

(1) Harris, P. J. F. *Carbon Nanotubes and Related Structures: New Materials for the Twenty-First Century*; Cambridge University Press: Cambridge, U.K., 1999.
(2) Iijima, S. *Nature* **1991**, *354*(6348), 56–58.
(3) Chen, J.; Perebeinos, V.; Freitag, M.; Tsang, J.; Fu, Q.; Liu, J.; Avouris, P. *Science* **2005**, *310*(5751), 1171–1174.
(4) Blase, X.; Rubio, A.; Louie, S. G.; Cohen, M. L. *Europhys. Lett.* **1994**, *28*(5), 335–340.
(5) Miyamoto, Y.; Rubio, A.; Cohen, M. L.; Louie, S. G. *Phys. Rev. B* **1997**, *50*(7), 4976–4979.
(6) Ishigami, M.; Sau, J. D.; Aloni, S.; Cohen, M. L.; Zettl, A. *Phys. Rev. Lett.* **2005**, *94*(5), 056804–4.
(7) Chopra, N. G.; Luyken, R. J.; Cherrey, K.; Crespi, V. H.; Cohen, M. L.; Louie, S. G.; Zettl, A. *Science* **1995**, *269*(5226), 966–967.
(8) Yu, D. P.; Sun, X. S.; Lee, C. S.; Bello, I.; Lee, S. T.; Gu, H. D.; Leung, K. M.; Zhou, G. W.; Dong, Z. F.; Zhang, Z. *Appl. Phys. Lett.* **1998**, *72*(16), 1966–1968.
(9) Arenal, R.; Stephan, O.; Cochon, J. L.; Loiseau, A. *J. Am. Chem. Soc.* **2007**, *129*(51), 16183–16189.
(10) Han, W.; Bando, Y.; Kurashima, K.; Sato, T. *Appl. Phys. Lett.* **1998**, *73*(21), 3085–3087.
(11) Lourie, O. R.; Jones, C. R.; Bartlett, B. M.; Gibbons, P. C.; Ruoff, R. S.; Buhro, W. E. *Chem. Mater.* **2000**, *12*(7), 1808–1810.
(12) Kim, M. J.; Chatterjee, S.; Kim, S. M.; Stach, E. A.; Bradley, M. G.; Pender, M. J.; Sneddon, L. G.; Maruyama, B. *Nano Lett.* **2008**, *8*(10), 3298–3302.
(13) Tang, C.; Bando, Y.; Sato, T.; Kurashima, K. *Chem. Commun.* **2002**, *12*, 1290–1291.
(14) Zhi, C.; Bando, Y.; Tan, C.; Golberg, D. *Solid State Commun.* **2005**, *135*(1−2), 67–70.
(15) Chen, H.; Chen, Y.; Liu, Y.; Fu, L.; Huang, C.; Llewellyn, D. *Chem. Phys. Lett.* **2008**, *463*(1−3), 130–133.
(16) Oku, T.; Narita, I.; Tokoro, H. *J. Phys. Chem. Solids* **2006**, *67* (5−6), 1152–1156.
(17) Bechelany, M.; Bernard, S.; Brioude, A.; Cornu, D.; Stadelmann, P.; Charcosset, C.; Fiaty, K.; Miele, P. *J. Phys. Chem. C* **2007**, *111* (36), 13378–13384.
(18) Zhi, C.; Bando, Y.; Tang, C.; Xie, R.; Sekiguchi, T.; Golberg, D. *J. Am. Chem. Soc.* **2005**, *127*(46), 15996–15997.
(19) Zhi, C.; Bando, Y.; Tang, C.; Golberg, D. *J. Am. Chem. Soc.* **2005**, *127*(49), 17144–17145.

 Published on Web 01/13/2010

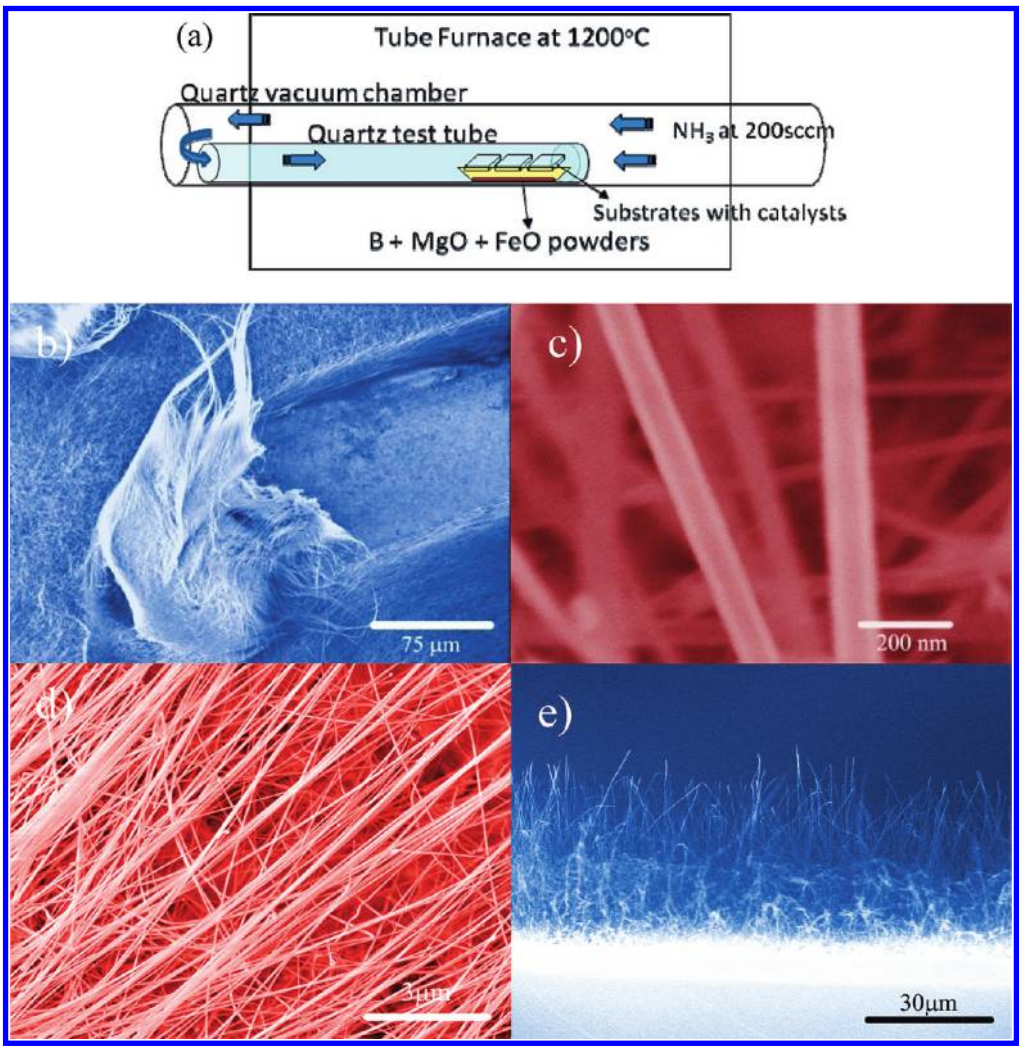

Figure 1. (a) Experimental layout. (b) Typical SEM images of the as-grown sample. Dense BNNTs can be scratched off from the sample. (c) High-magnification SEM showing the hollow center channel of a tube structure. (d) Dense BNNTs film on a Si substrate after slight compression. The diameter and length of the tubes is estimated to be 15−100 nm, and > 10 μm, respectively. (e) Cross-sectional view: Partially vertical-aligned BNNTs. (Artificial color was added to the SEM images.)

technique at 600 °C.[20] However, the length of BNNTs grown by this approach is still too short (up to ~600 nm) for most applications. We have then devoted our efforts to establish effective growth technique that enable the growth of long BNNTs in a resistive horizontal tube furnace, which is widely used for the synthesis of CNTs[21] and ZnO nanostructures.[22]

Lately, we have succeeded in growing BNNTs in such a conventional tube furnace by CVD at 1100−1200 °C.[23] This was obtained on the basis of our growth vapor trapping (GVT) mechanism and the BOCVD chemical route. We have shown that long BNNTs can be grown directly on Si substrates. We determined the band gap of BNNTs to be ~5.9 eV, higher than those grown by an induction furnace (~5.5 eV).[24] Although this success had provided a convenient technique for growing BNNTs in a conventional tube furnace, the approach was a spontaneous nucleation process with no control on the quality and growth location of BNNTs. Sub-band defect levels were still detected from our products at 4.78 and 3.7 eV. In addition, there is no CVD approach that enables the growth of BNNTs at desired growth locations and directions as commonly demonstrated for CNTs and nanowires. All these shortcomings are due to the fact that the actual catalysts that induce the growth of BNNTs on substrates are not clearly identified.

Here we report that MgO, Ni, and Fe were the active catalysts that enabled patterned growth of BNNTs directly on Si substrates using the GVT approach (Figure 1a). An Al_2O_3 underlayer (30 nm) was initially coated on a Si or SiO_2 substrate by pulsed-laser deposition. Subsequently, a thin film layer of MgO (15−30 nm), Ni, or Fe (10 nm) was deposited on the top of the Al_2O_3 layer. For

(20) Wang, J.; Kayastha, V. K.; Yap, Y. K.; Fan, Z.; Lu, J. G.; Pan, Z.; Ivanov, I. N.; Puretzky, A. A.; Geohegan, D. B. *Nano Lett.* **2005**, *5* (12), 2528–2532.
(21) Kayastha, V. K.; Wu, S.; Moscatello, J.; Yap, Y. K. *J. Phys. Chem. C* **2007**, *111*(28), 10158–10161.
(22) Mensah, S. L.; Kayastha, V. K.; Ivanov, I. N.; Geohegan, D. B.; Yap, Y. K. *Appl. Phys. Lett.* **2007**, *90*(11), 113108–3.
(23) Lee, C. H.; Wang, J.; Kayatsha, V. K.; Huang, J. Y.; Yap, Y. K. *Nanotechnology* **2008**, *19*(45), 455605.
(24) Jaffrennou, P.; Barjon, J.; Lauret, J. S.; Maguer, A.; Golberg, D.; Attal-Trétout, B.; Ducastelle, F.; Loiseau, A. *Phys. Status Solidi B* **2007**, *244*(11), 4147–4151.

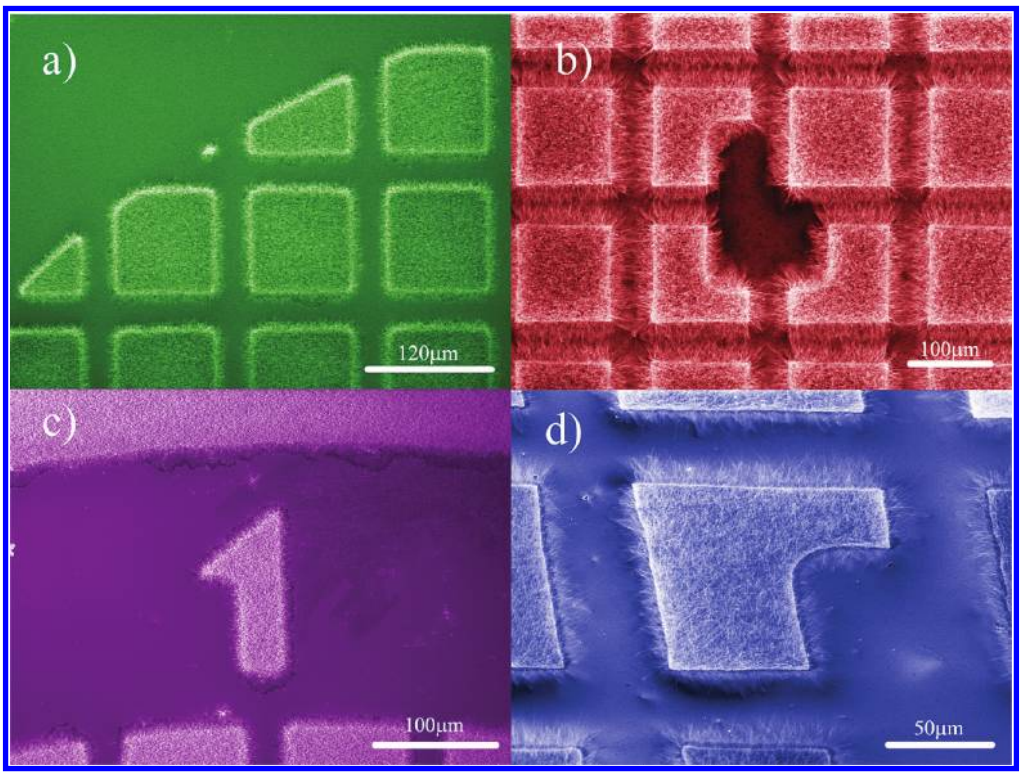

Figure 2. Demonstration of well-defined patterned growth of BNNTs on a substrate. (Artificial color was added to the SEM images.)

demonstrating the pattern growth of BNNTs, shadow masks (150 and 200 mesh) were used to define the location of catalysts. These substrates were then transferred to the thermal-CVD system for the growth of BNNTs. The growth procedures are presented in the Experimental Section.

Experimental Methods

Growth of BNNTs. MgO films of 10−30 nm were coated on Si substrates by a pulsed laser deposition (PLD) technique. These substrates were then placed on the top of an alumina combustion boat in which B, MgO, and FeO precursors (molar ratio of 4:1:1) filled the inside of the boat. This setup was loaded inside a closed-end quartz tube in the horizontal tube furnace with the catalytic films facing upward. The precursors and substrates were then heated up to 1100−1200 °C with an ammonia flow of 200−350 sccm and kept for ~30 min. As shown in Figure 1a, growth vapor trapping (GVT) is obtained at the closed end of the quartz test tube without being affected by the flow of the ammonia gas.[23]

Patterned Growth of BNNTs. TEM copper grids were used as the shadow masks and mounted on the substrate by adhesive tapes. A 30 nm thick Al_2O_3 film was then deposited by PLD, followed with a 10 nm thick MgO, Ni, or Fe film. The TEM grid was then removed after the deposition. These substrates were then transferred to the CVD system for the synthesis of BNNTs.

Results and Discussion

Typical morphology of the as-grown BNNTs film was examined by scanning electron microcopy (SEM) as shown in Figure 1b. A high magnification SEM (Figure 1c) reveals a hollow center channel of a tube structure. These BNNTs have a typical diameter of 60 nm. The average lengths of the BNNTs are more than 10 μm. These BNNTs always grow partially vertically aligned to the substrate surface, as revealed from the cross-section view (Figure 1e). It is worth noting that these vertically aligned BNNTs exhibit superhydrophopic behaviors and are applicable as transparent, self-cleaning anticorrosive coatings.[25] A light mechanical compression can make these BNNTs horizontally laid on the substrates as shown in Figure 1d. The superhydrophopic behaviors of BNNTs will be briefly reduced in such a case. As shown in Figure 2, well-defined patterns of BNNTs can be deposited using our approach. This implies that the chemical reaction between the spatially predefined catalysts (MgO, Ni, or Fe) and the reactive growth species from the combustion boat (B_2O_2 or BN vapors) plays an important role in the growth of BNNTs as follows

$$B_2O_2(g) + MgO(s) + 2NH_3(g) \rightarrow 2BN(BNNTs) + MgO(s) + 2H_2O(g) + H_2(g) \quad (1)$$

$$\text{Or, } B_2O_2(g) + Ni/Fe(s) + 2NH_3(g) \rightarrow 2BN(BNNTs) + Ni/Fe(s) + 2H_2O(g) + H_2(g) \quad (2)$$

The generation of B_2O_2 vapors from the combustion boat was previously described[13] as

$$2B(s) + 2MgO(s) + FeO(s) \rightarrow B_2O_2(g) + 2Mg(s) + Fe(s) \quad (3)$$

BNNTs can be easily collected from the substrates by mechanical scratching or extracted into suspension by

(25) Lee, C. H.; Drelich, J.; Yap, Y. K. *Langmuir* **2009**, *25*(9), 4853–4860.

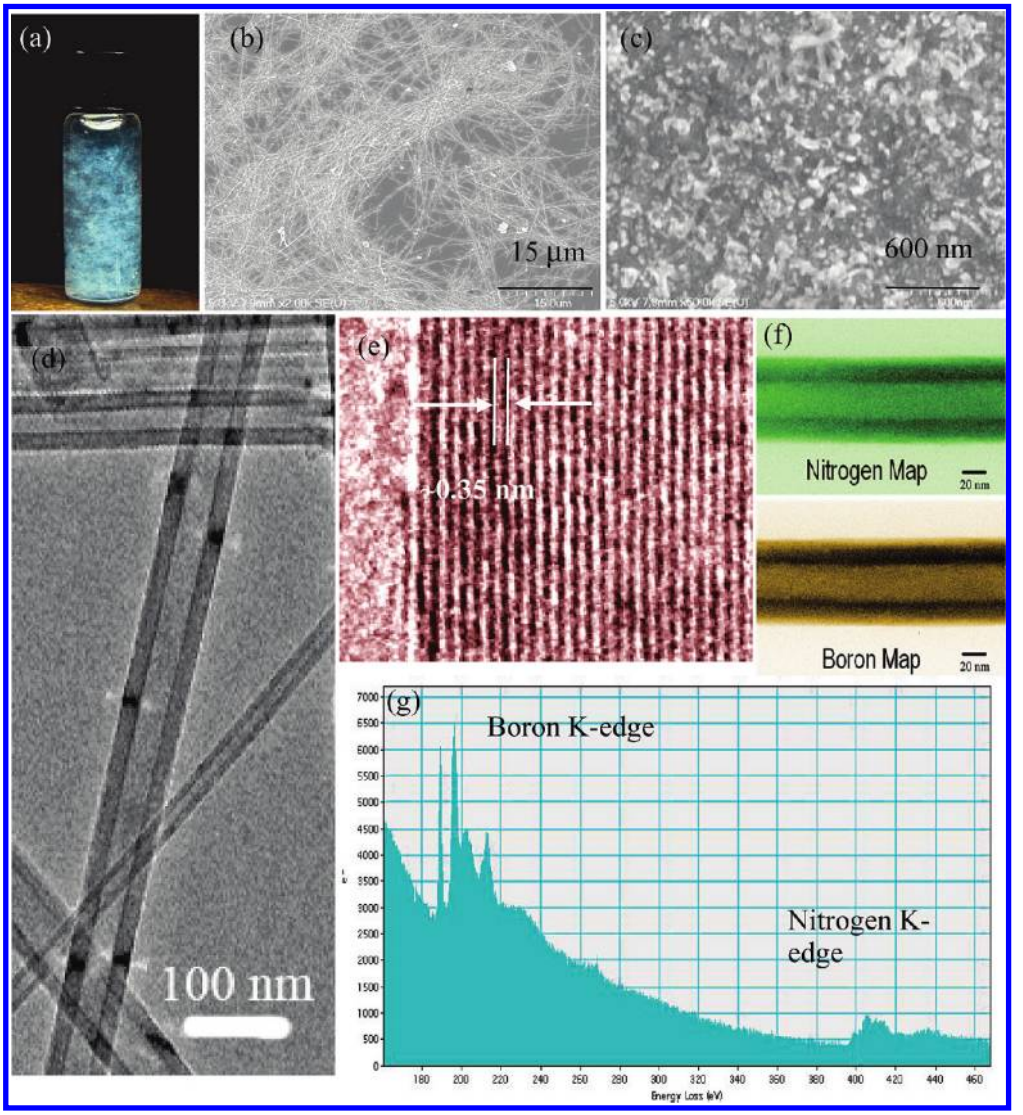

Figure 3. (a) BNNTs suspended in ethanol as extracted by ultrasonication of the as grown samples. (b) Clean BNNTs redeposited on fresh substrates are readily used for device applications. (c) Catalytic particles remained on the substrates after the extraction of BNNTs. (d) TEM images showing nanotubular structures of BNNTs with amorphous-free side-walls. (e) The interlayer distance of BN shells is estimated as ~0.35 nm. (f) Energy filtered imaging of an individual BNNT and (g) the EELS spectra of BNNTs.

ultrasonic bath. Whitish BNNT suspension will be formed with no sign of precipitation for longer than 2 weeks (Figure 3a). This BNNT suspension can be used for UV−visible spectroscopy, TEM, and devices. Clean BNNTs can also be redeposited onto fresh substrates using the same suspension (Figure 3b). Catalytic particles are left on the substrates (Figure 3c). Transmission electron microscopy (TEM) reveals that these BNNTs have good nanotubular structures (Figure 3d), consistent with the high-magnification SEM image. High-resolution TEM (Figure 3e) suggests that the as-grown BNNTs are well-crystallized, with side walls that are much cleaner (no amorphous BN coatings) than our samples grown without using catalytic films.[23] The interlayer spacing of the BNNTs wall was estimated as ~0.35 nm, slightly larger than that of h-BN bulk crystals (~0.33 nm). From these SEM and TEM analyses, we seldom found residual catalyst particles on BNNTs. This suggests that the growth of these BNNTs is following the base-growth mode, as confirmed by the particles left on the substrates after the extraction of BNNTs by sonication bath. Energy-filtered imaging and electron energy loss spectroscopy (EELS) indicate that these BNNTs consist of B and N atoms with a ratio of 1:1 (Figure 3f,g).

The as-grown BNNT samples were also characterized by Raman and Fourier transformed infrared (FTIR) spectroscopy. Raman spectra were collected as excited by a HeCd (λ = 325 nm) laser. A sharp Raman peak at ~1367 cm^{-1} was detected (Figure 4a), which corresponds to the E_{2g} in-plane vibrational mode of the h-BN networks. The FTIR spectra were taken in a transmission mode on BNNTs dispersed on a thin Si substrate under a FTIR microscope. As shown in Figure 4b, three absorption frequency regimes can be obviously distinguishable at ~807, ~1369, and ~1532 cm^{-1}. The absorption band at ~1369 cm^{-1} is attributed to the in-plane stretching modes of the h-BN networks that vibrates along the longitudinal (L) or tube axis of a BNNT. The absorption band at ~1532 cm^{-1} is assigned to the stretching of the h-BN network along the tangential (T) directions of a

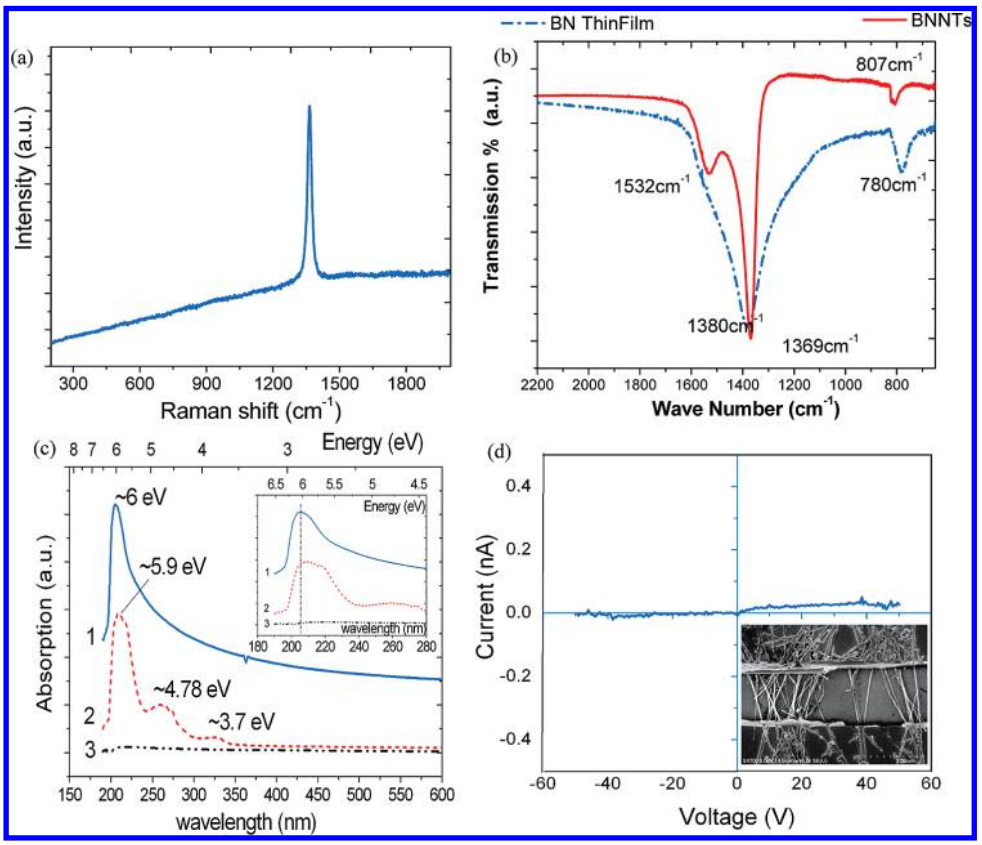

Figure 4. (a) Raman and (b) FTIR spectra of BNNTs. (c) UV−visible absorption spectra taken from BNNT suspensions and ethanol (spectra 1, BNNTs grown with catalyst films; spectra 2, BNNTs grown without catalyst films; spectra 3, ethanol). (d) A bunch of BNNTs connected across two microelectrodes (inset) showing no significant current flows at bias voltages from −50 to 50 V.

BNNT (around the circumference of nanotubes). It is also worth noting that this stretching mode smears out for h-BN bulks or thin films, and only shows up when the tube curvature induces an anisotropic strain on the h-BN networks. Thus, we suggest that only highly crystalline BNNTs would show up this stretching mode. The weak absorption at ~807 cm^{-1} is associated to the out-of-plane radial buckling (R) mode where boron and nitrogen atoms are moving radially inward or outward. All these optical spectra are the fingerprints of BNNTs.[23]

UV−visible absorption spectroscopy was used to characterize our BNNTs (suspended in ethanol). A strong absorption band centered at 205 nm was detected, indicating a band gap of ~6.0 eV (spectra 1 in Figure 4c). This band gap is slightly larger than what we reported (spectra 2) for BNNTs grown without using catalyst films.[23] As shown, the 4.78 and 3.7 eV absorption shoulders detected in our previous measurements (spectra 2) now disappeared. This means the use of MgO catalytic films has reduced the defect levels in the BNNTs. The spectra taken from ethanol (spectra 3) are shown together for comparison. We further conducted electrical transport measurement on a bunch of BNNTs (Figure 4d). 60 nm Au on the top of 20 nm Cr was used as the microelectrodes (100 μm × 100 μm). No electrical current was detected within the range of ±50 V. This shows that our BNNTs are good insulators at room temperature, as expected from the wide energy band gap of these nanomaterials.

Among the three catalysts suggested here, MgO is the most effective catalyst for producing dense BNNT thin films with well-defined patterns. It is also important to have the Al_2O_3 buffer layer under the catalyst films. Our results indicate that all the tested catalysts can react with the Si substrates and lost their catalytic properties. Thus the Al_2O_3 buffer layer functions as the diffusion barrier that prevent the catalysts from react with the substrates. For the patterned growth reported here, we let the reactive growth species generated from the precursor powders to react solely with the patterned catalyst to form BNNTs according to eqs 1 and 2. Therefore, we have reduced the contents of MgO in the precursor powders in order to suppress spontaneous nucleation and growth of BNNTs on the substrates. We have also let the catalyst films to face upward instead of facing to the precursor powders (Figure 1a). All these procedures have prevented the spontaneously grown BNNTs from coating on the substrate surface without following the patterns of the catalyst. This is a controlled catalytic CVD (CCVD) approach instead of spontaneous nucleation and growth of BNNTs from the precursor powders as previously demonstrated.[13,14,23] From the TEM results, we can hardly find any Mg or MgO based fillings inside the tube, unlike previously reported.[26] We propose that all the process and parameters demonstrated here are

(26) Golberg, D.; Bando, Y.; Mitome, M.; Fushimi, K.; Tang, C. *Acta Mater*. **2004**, *52*(11), 3295–3303.

important for producing high-quality BNNTs. It is also believed that the upward flows of these growth species are responsible for the growth of partially vertically aligned BNNTs. For the case when MgO was used as the catalyst, there is a small possibility for MgO to form MgN_2, MgB_2, or other Mg−B−N ternary compounds during the growth process. These intermediate phases are not detected by Raman, FTIR, and X-ray diffraction in our samples. This argument is also supported by the detection of MgO-based nanowires filling in BNNTs.[26]

Conclusions

In summary, we have established a simple growth vapor trapping (GVT) approach for patterned growth of high-quality BNNTs by catalytic CVD. These BNNTs are always partially vertical aligned on Si substrates at desired locations using patterned MgO, Ni, or Fe catalytic films. The as-grown BNNTs have a band gap of ~6.0 eV without significant sub-band absorption centers. This was further verified by current−voltage measurements, which suggest that our BNNTs are perfect insulators, as consistent to their wide energy bandgap property. Following this success, the growth of BNNTs is now as convenient as growing CNTs and ZnO nanowires. Pattern growth not only explains the role of catalysts in the formation of BNNTs, but this work could be of important for future device fabrication.

Acknowledgment. This project is supported by National Science Foundation CAREER award (Award 0447555), the U.S. Department of Energy, the Office of Basic Energy Sciences (Grant DE-FG02-06ER46294), and the Electron Microscopy Center (Project 080512-01A) at Argonne National Laboratory.